AL.2.1999-150
C.2

Forest Development Research

PROGRAM

Manning Diversified Forest Products
Research Trust Fund
MDFP12/97
MIXLIGHT: A Flexible Light
Transmission Model for Mixed-species
Forest Stands – Final 1997/98

Alberta
ENVIRONMENTAL PROTECTION

Manning Diversified Forest Products
Research Trust Fund
MDFP12/97

MIXLIGHT: A Flexible Light Transmission Model for Mixed-species Forest Stands – Final 1997/98

September 1998

By Kenneth J. Stadt and Victor J. Lieffers
Department of Renewable Resources
University of Alberta
Edmonton, Alberta
Canada

Pub. No. T/429
ISBN: 0-7785-0401-8

- Disclaimer -

The study on which this report is based was funded by the Manning Diversified Forest Products Research Trust Fund (MDFP) which is a component of Alberta's Environmental Protection and Enhancement Fund (EPEF). The views, statements and conclusions expressed, and the recommendations made in this report are entirely those of the author(s) and should not be construed as the statements conclusions, or opinions of members of the Manning Diversified Forest Products Research Trust Fund or of the Government of Alberta and its EPE Fund.

Abstract

MIXLIGHT: A Flexible Light Transmission Model for Mixed-Species Forest Stands

by

Kenneth J. Stadt and Victor J. Lieffers

We describe the calibration and structure of a multi-species, multi-scale light transmission model, MIXLIGHT, and demonstrate its effectiveness for predicting instantaneous light availability at the canopy scale across a wide range of forest stand compositions, seasons, and weather conditions. MIXLIGHT uses the Beer-Lambert Law to calculate transmission at the canopy or crown scale using standard forest inventory data and two other parameters, foliage area density and foliage inclination. A simple and rapid method of calibrating these parameters for the species of interest is presented, using direct-beam light transmission measurements made in the shadows of freshly isolated trees. With this information, MIXLIGHT predicted light transmission at the stand level closely for 17 forest inventory plots with a wide range of density and species composition, during leaf-on and leaf-off seasons and under sunny and cloudy conditions (n=25, r=0.86). Implications of using partial and coarse-scale data sets in MIXLIGHT are evaluated with a sensitivity analysis. Since MIXLIGHT is based on the individual tree, it allows for simple manipulation of stand structure to study the effects of silvicultural options on light availability. The two modeling scales allow the input of various kinds of data, allowing predictions from data of different sources and completeness. We believe MIXLIGHT will provide an accessible and effective tool for forest regeneration planning and stand management.

Acknowledgements

Funding for this research was provided by Manning Diversified Forest Industries. The authors wish to thank Susan Hayduk, David Kelsberg, and Bradley Pinno for field assistance; Tim Vinge of Canadian Forest Products Hines Creek Division, Kent MacDonald and Roger Hayward of Foothills Model Forest and Darin Leadley of Weyerhauser Canada's Drayton Valley Division for site locations and information. Thanks also to Christian Messier and Ernest Lo for helpful discussions, and Glen VanBrummelen for mathematical assistance.

Table of Contents

DISCLAIMER i
ABSTRACT ii
ACKNOWLEDGEMENTS iii
TABLE OF CONTENTS iv
LIST OF FIGURES AND TABLES v
INTRODUCTION 1
MATERIALS AND METHODS 4
Overview 4
Theory 4
Study Area 6
Model Calibration 6
The MIXLIGHT Model 12
Stand-Level Validation 15
Model Sensitivity and Foliage Inclination 16
RESULTS 18
Calibration 18
Validation 19
Sensitivity Analysis and Foliage Inclination 20
DISCUSSION 23
CONCLUSIONS 27
LITERATURE CITED 28
APPENDIX A 31

List of Figures and Tables

Figure 1. Calibration of foliage area density and foliage inclination parameters in the shadow of individual trees 8

Figure 2. MIXLIGHT stand-level validation 20

Figure 3. Sensitivity analysis of the foliage area density, foliage inclination, and crown length and radius parameters 21

Figure 4. MIXLIGHT stand-level validation with foliage inclination assumed to be spherical 22

Table 1. Calibration trees' bole and crown parameters 19

Introduction

The characterization of light in forests has been a key focus of work on forest community dynamics and regeneration. Numerous studies have established the dependence of tree and understory growth on available light in stands (Messier et al. 1989, Lieffers and Stadt 1994) and microsites (Poulson and Platt 1989, Alaback and Tappeiner 1991, Klinka et al. 1992, McLure and Lee 1993, Poage and Peart 1993, Runkle et al. 1995). However, adequate measurement of light is time-consuming due to the diurnal and seasonal changes in solar position, heterogeneity in space and composition of the canopy, and leaf-on and off cycles. A number of authors have shown that it is possible to use the well-described laws of solar geometry and information about the canopy structure to predict light regimes in forests on the stand (Norman and Jarvis 1975) and the microsite level (Grace et al. 1987, Wang and Jarvis 1990, Pukkala et al 1993, Canham et al. 1994, Cescatti 1997b, Ter-Mikaelian et al. 1997).

Forest tenures often cover large areas of mixed composition and have varying amounts of inventory data available for management decisions. There is also a considerable range of stand-tending and harvesting options, from unmanaged to intensive thinning and partial-cut silvicultural systems, all of which have implications for the light regime and vegetation response. Clearly, there is a need for an easily-calibrated, multi-species model of light availability that is flexible enough to produce accurate understory light predictions on a scale appropriate to the inventory data and management goals. Such a model would be of considerable help in studying, planning and managing regeneration in working and research forests (Lieffers et al. 1998).

Light availability models developed for forests vary considerably in approach and complexity. The simplest fit the Beer-Lambert Law empirically, calculating light transmission based on the overlying leaf area index and an extinction coefficient (Monsi and Saeki 1953, Jarvis and Leverenz 1983, Pierce and Running 1988). These produce reasonable predictions only for a restricted range of solar angles and are limited to stands which are similar to those in which their extinction coefficients were calibrated (Lieffers et al. 1998). Another approach has been to model the canopy as a number of layers of grouped foliage, each with an appropriate fraction of the canopy leaf

area, a layer transmission and a layer reflection coefficient. Such a model predicted the light profile well in a pure Sitka spruce plantation (Norman and Jarvis 1975), but a considerable amount of data is required to generate the model parameters. These foregoing models generate a light profile with height only, and do not account for the horizontal spatial variation of light through the stand. A spatial approach is to group foliage into identifiable objects such as rows, crowns, crown layers or shoots which are described geometrically as cylinders, ellipsoids, disks, or irregular polyhedrals in three-dimensional space. Light penetration through these objects is modeled spatially and temporally, given the solar geometry for that latitude and time, and the position and size parameters of the array of shapes. Pukkala et al. (1993) tested a crown model of this type in a pure Scots pine stand and Canham et al. (1994) and Ter-Mikaelian et al. (1997) developed models for mixed-species stands. These use measurements of the projected leaf area density within the crown or a similar extinction coefficient to compute through-crown light transmission. They do not account for light reflection, but are able to predict the spatial distribution of light at microsites throughout the stand with some degree of accuracy. Lastly, there are models which combine the spatial features of the geometric approach with a layer model for dealing with light reflection (Grace et al. 1987, Wang and Jarvis 1990, Cescatti 1997a). These have shown excellent spatial accuracy in pure stands, but require a suite of detailed input data.

Tools for modeling light are thus well-developed. Applications, however, have been limited by model inflexibility or the quantity and type of data required. Calibration has been particularly difficult. For our model, MIXLIGHT, we aimed to build a flexible, accessible simulator which would allow light penetration theory to be applied to existing forest inventory data with minimal calibration and make light availability predictions for a wide range of forest stands. We designed MIXLIGHT to operate at either the crown or canopy scale to fit the data available and the spatial precision required. Since the individual tree is the basic forest inventory and harvested unit, MIXLIGHT can generate light predictions from either a complete tree list (an inventory of every tree in the plot) or a minimal list of species stem densities and bole diameter distribution. A complete list includes species, diameter, height, height to the base of the live-crown, crown radius, and tree location coordinates. Where some of this information is missing, regressions are used to determine these parameters. A separate table of foliage area densities, foliage inclination

distribution parameters and the crown shape for each species and crown-class is required; these can be obtained following the calibration described here or from other sources. To account for exposure effects, stand slope and aspect are also required. When the tree position data are missing, the inventoried stand is small (dominated by edge effects) or if only a stand-level estimate of light is required, MIXLIGHT operates at the canopy scale, generating canopy parameters from the tree data. Since canopy parameters can also be obtained from remote-sensing or canopy analysis instruments, the capability to predict stand-level light directly from canopy leaf area index and inclination information is also available.

In this paper, we describe a simple method of calibrating the foliage area density and inclination coefficients which drive the model, present the structure of MIXLIGHT, and validate its stand-level predictions across a wide range of stand types in the boreal mixedwood forest of central Alberta, Canada. The ability of MIXLIGHT to predict light availability with more limited inventory data is also demonstrated with a reduced set of data and a sensitivity analysis.

Materials and Methods

Overview

The species-specific crown shape, foliage area density and inclination distribution parameters that drive MIXLIGHT are calibrated from measurements of direct-beam light transmission and crown size made in the shadows of isolated residual trees in cutblocks (Fig. 1). Sunbeams are used as thin, parallel probes, and the Beer-Lambert Law (Eqn. 1) is inverted to estimate the foliage area density and inclination distribution. These parameters are then applied to other stands for modeling light transmission. For crown-scale modeling, a list of tree positions, bole and crown dimensions is read. The foliage area density and inclination parameters are applied to the appropriate species, and the Beer-Lambert Law (Eqn. 2) used to determine light transmission along rays extending from the sun and sections of sky to the measurement point. Intersection points with each crown or bole, and the path length through these, are determined by the solving the intersection of the ray with the geometric crown or bole. Transmission along each ray is weighted appropriately to yield a light transmission prediction for that point. Canopy scale modeling is similar except there is only one region (the canopy) to intersect the light rays. Canopy foliage area density and foliage projection are calculated from the tree list (unless supplied directly), weighting by the bole and foliage surface area of each species.

Theory

Light transmission through the canopy or crown is modeled assuming random foliage distribution within the crown or canopy region. By 'light,' we specifically mean photosynthetically active radiation (400-700 nm). 'Foliage' here is taken to include leaves and the branches and bole that are contained within the crown volume since these all attenuate light. Foliage is also assumed to incline from the horizontal as the surface area of an ellipsoid (Campbell and Norman 1989). Each bit of foliage area is assumed to transmit and reflect no light so that a thin ray of light incident on a crown or canopy is either completely absorbed or completely transmitted, depending on whether it hits or misses foliage. Over an area at least ten times the average foliage element's size, the

probability that the ray will not be intercepted is equal to the measured direct-beam light transmission (below ÷ above canopy light) (Lang and Xiang 1986).

The probability that a thin ray will not be absorbed by random foliage in the crown array or a canopy ($P(0)$, Eqn. 1) is given by the Poisson distribution (Horn 1971, Lang and Xiang 1986), but the same assumptions underlie the Beer-Lambert Law (Swinehart 1955). Equation 2 is rearranged to yield light flux density ($q[Z, \alpha]$) rather than transmission (T), which is a more convenient form for modeling the diffuse light flux.

[1] $$P(0) = T = \frac{q[Z,\alpha]}{q_0[Z,\alpha]} = e^{-\sum_{j=1}^{n} G[Z,x_j]S_j F_j}$$

[2] $$q[Z,\alpha] = q_0[Z,\alpha] e^{-\sum_{j=1}^{n} G[Z,x_j]S_j F_j}$$

In these equations, $q[Z, \alpha]$ is the flux density of a single ray of light through a surface perpendicular to the ray direction, originating from a distant point source defined by its zenith (Z, angle from vertical) and azimuth (α, compass orientation), $q_0[Z, \alpha]$ is the light incident above the canopy from the same source, $G[Z,x_j]$ is the projection or shadow area of a unit area of foliage (unitless) perpendicular to the direction of the light source, x_j is a parameter describing the foliage area inclination (see below), S_j is the path length (m) through the light-absorbing region, and F_j is the foliage area density (in m^2m^{-3}). The product $G[Z,x_j]S_jF_j$ is the absorbance for the region j. Since absorbances are additive, the summation in Eqns. 1 and 2 deals with any number of light absorbing regions (n) that intersect the light path, from a single canopy (n = 1) to an array of individual crowns (n = number of trees). For instantaneous estimates of light transmission, Eqn. 2 is applied once for direct-beam radiation transmission (T_{direct}) using the solar position angles (Z_s, α_s; Eqn. 3a), and multiple times to equal-area sectors of the sky for integrating the transmission of diffuse skylight (Eqn. 3b). The flux densities of all rays are cosine-corrected to the flux density through a horizontal surface. For daily or seasonal transmission, a "seasonal sky" is developed which adds to the diffuse skylight irradiance the irradiance from the sun while it passes through each sky sector and is not obscured by cloud. Eqn. 1 is then applied multiple times, using the Z, α coordinates of each of these sectors and the incident seasonal light flux density ($q_0[Z, \alpha]$)

calculated for the sector (Eqn. 3b). With this approach, MIXLIGHT can calculate light availability seasonally as well as at any time of day in any season during sunny or overcast conditions.

[3a] $$T_{direct} = \frac{Q_{direct}}{Q_{0,direct}} = \frac{\cos Z_s \; q[Z_s, \alpha_s]}{\cos Z_s \; q_0[Z_s, \alpha_s]}$$

[3b] $$T_{diffuse,\,daily\,or\,seasonal} = \frac{Q}{Q_0} = \frac{\int_{\cos Z=1}^{0} \int_{\alpha=0}^{2\pi} \cos Z \; q[Z,\alpha] \, d\alpha \, d\cos Z}{\int_{\cos Z=1}^{0} \int_{\alpha=0}^{2\pi} \cos Z \; q_0[Z,\alpha] \, d\alpha \, d\cos Z} \cong \frac{\sum_{c=1}^{nc} \sum_{a=1}^{na} (\cos Z_c \; q[Z_c, \alpha_a])}{\sum_{c=1}^{nc} \sum_{a=1}^{na} (\cos Z_c \; q_0[Z_c, \alpha_a])}$$

In Eqn. 3b, c=1..*nc* is the index for the zenith angles which are divided into *nc* equal increments of the cosine of the zenith from 1 (Z=0) to 0 ($Z=\frac{\pi}{2}$) to achieve equal-area sampling), and a=1..*na* is the azimuth angle index, divided into *na* equal increments from 0 to 2π.

Study area

Calibration and validation of MIXLIGHT were performed in a number of stands across west-central Alberta (53°30' - 54°10' N, 114°50' - 118° W). Mean annual temperature in this region is 0.9 - 2.6°C, and precipitation is 530 - 560 mm a^{-1}, approximately 60% of it falling during the growing season (May - August) (Anon. 1982a, 1982b). All stands were upland sites with submesotrophic to mesotrophic nutrient status and mesic to hygric ecological moisture regime (Anon. 1991)

Model Calibration

Field sites

The crown properties of various tree species were determined on newly-isolated residual trees on clearcut edges and in partial-cut stands. We visited 10 cutblocks from late June to August in 1996 and 1997 for leaf-on calibration, and in April of 1997 for leaf-off measurements. Before cutting, the sites were dominated by either aspen (*Populus tremuloides* Michx.), white spruce (*Picea glauca* (Moench) Voss) or mixtures of these, balsam fir (*Abies balsamea* (L.) Mill.), balsam poplar (*Populus balsamifera* L.), and white birch (*Betula papyrifera* Marsh.). Trees were

measured as soon after logging as possible so they still retained the leaf and shape characteristics they had while growing in the stand.

Crown sampling

Light measurements were taken with an 80 sensor, 80 × 1 cm linear quantum radiometer (Model SF-80, Decagon Devices, Inc., Pullman, WA), which measures photosynthetic photon flux density (PPFD). Measurements were made during periods of direct sun when the trees cast a clearly delineated shadow on the ground.

Crown size and direct sunlight transmission measurements were made in single-crown shadows which did not overlap with other shadows. At each sample tree, total shadow length (h_t', stem base to shadow apex), length to the base of the shadow's live-crown (h_{lc}') and time of measurement were recorded first (Fig. 1a). The light sampling strategy depended on the crown shape. Parallel transects at 1-2 m spacing (depending on crown size) perpendicular to the central axis of the crown (see Fig. 1a) were used for conical, cylindrical, paraboloid and rocket-shaped crowns. Eight radial transects at 45° intervals originating from the center of the crown shadow were used to sample ellipsoidal crowns (Fig. 1b). To compensate for the lateral movement of the sun (0.25° min^{-1}), the origin of each transect was aligned with the central axis of the stem shadow before commencing each transect. Vertical changes in the sun's position ($<0.1^{\circ}$ min^{-1}) were small enough to be ignored during the sampling period. Where necessary, ground slope and aspect were measured to transform the transect positions to horizontal coordinates. Every 50 cm from the origin, the radiometer wand has held at right angles to the transect (Fig. 1c), six light measurements taken over six seconds and the average recorded. Sampling extended 100-150 cm past the edge of the shadow to provide at least one unshaded light measure for that transect. Transect length (d, Fig. 1c) from the crown center to the shadow edge was recorded for shape determination. Total (Q_0) and diffuse light ($Q_{diffuse}$) were measured in full sun adjacent to the crown shadow immediately before and after sampling each tree by exposing then shading the tip sensor of the radiometer with a 20 cm disk at 2 m distance, and recording the output from that single sensor. Sampling time depended on tree size, but was generally less than 20 minutes per tree.

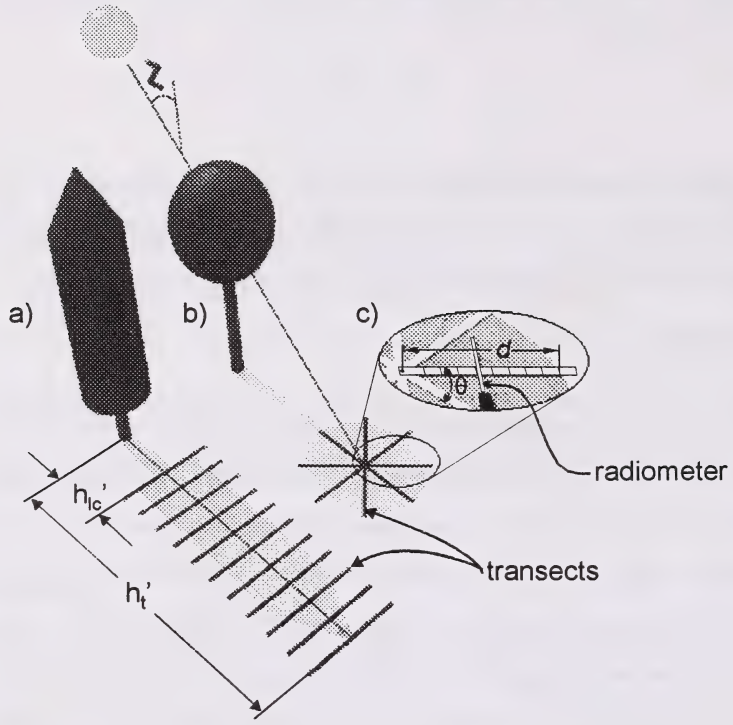

Figure 1. Calibration of foliage area density and foliage inclination parameters in the shadow of individual trees. a) Transect layout for rocket (shown), cylindrical, paraboloid and conical crowns. Transects originate at the central axis of the shadow and extend perpendicularly in both directions to the shadow edge. Measurements of shadow height (h') and shadow height to live-crown (h_{lc}') are shown. b) Transect layout for ellipsoidal crowns. Transects originate in the center of the crown and extend to the shadow edge. The solar zenith angle (Z) and a ray of sunlight passing through the center of the crown are shown. c) Detail of a single transect showing the light measurement protocol with a radiometer wand held at right angles to the transect. Transect angle from the apex (θ) and the distance from the transect origin to the shadow edge (d) are also shown.

Crown shape and size

An appropriate geometric shape (ellipsoid, paraboloid, cone, cylinder, or rocket (cone perched on a cylinder)) was chosen for the crown of each species (Table 1, Results). Crown length and radius were calculated by assuming these 3-dimensional crowns cast equivalent 2-dimensional shadows, e.g. ellipsoidal crowns cast elliptical shadows, conical crowns cast triangular shadows, *etc*. For elliptical crown shadows, the crown radius (cr) and crown shadow length (cl') were determined by nonlinear least-squares regression of the polar equation for an ellipse, solved for transect length (distance from the transect origin to the shadow edge, d, Fig. 1c) *vs*. the transect

angle from the shadow apex (Θ, Fig. 1c), for the eight transects (Eqn. 4). For parabolas and triangular shadows, Eqns. 5 and 6 use the transect length (*d*) and transect 'height' (*h'*, the distance from the trunk to the origin of the transect along the central shadow axis, Fig. 1a) data to provide estimates of the crown radius at the 'height' of the shadow's live crown. These estimates of *cr* for all transects in a tree shadow were averaged to yield the best estimate of the tree's crown radius. In the shadows of rocket-shaped or cylindrical trees, *cr* was determined by averaging *d* for the transects between the base of the live crown and the top of the cylinder. The proportion of cone *vs.* cylinder was set as 25:75, based on visual examination of the crowns. Crown shadow length (*cl'*) for paraboloid, conical and rocket-shaped crowns was determined as the difference between tree shadow length (h_t') and length to the base of the shadow's live crown (h_{lc}').

[4] $$d = \sqrt{\frac{cr_{ellipsoid}^2 \left(cl'_{ellipsoid}/2\right)^2}{cr_{ellipsoid}^2 + \left[\left(cl'_{ellipsoid}/2\right)^2 - cr_{ellipsoid}^2\right]\sin^2\Theta}}$$

[5] $$cr_{paraboloid} = \sqrt{\frac{d^2\left(h_t' - h_{lc}'\right)}{h_t' - h'}}$$

[6] $$cr_{cone} = \frac{d\left(h_t' - h_{lc}'\right)}{h_t' - h'}$$

Actual tree height (h_t), height to the base of the live crown (h_{lc}) and crown length (*cl*) were determined by dividing these lengths measured or determined on the tree shadow by the tangent of the solar zenith (*Z*, Fig. 1b, Eqn. 7). In all cases, we assumed the crowns were horizontally circular in cross-section so that their crown radius was unaffected by solar angle. Equations for the solar zenith and azimuth at any time, day, latitude and longitude are given in Iqbal (1983).

[7] $$actual\ length = \frac{shadow\ length}{\tan Z}$$

Crown foliage area density

Light transmission and absorbance was determined for each point on each transect. The transmission of direct beam light was calculated by taking the difference between total light measured (*Q*) and diffuse light ($Q_{diffuse}$), and dividing this by the difference between total light

measured outside the crown shadow (Q_0) and diffuse light. Direct beam transmission was converted to absorbance (A, Eqn. 8).

[8] $$A = -\ln[(Q - Q_{diffuse})/(Q_0 - Q_{diffuse})]$$

The length of the light path through the crown (S) was estimated by determining the solar zenith at the time of measurement and solving for the intersection of the line described by the sun angle and the measurement point with the geometric crown. A Cartesian coordinate system was used, with the origin at the center of the crown shadow, the y-axis increasing toward the shadow apex, the x-axis increasing westerly, and the z-axis straight up. Equations for determining the intersection points ($P_1(x_1, y_1, z_1)$ and $P_2(x_2, y_2, z_2)$) for a ray passing through the various crown shapes were generated by simultaneously solving the line equation with the equation for each of these geometric shapes (see Appendix A). If the intersection points were complex numbers, the ray lay completely outside the crown with no real number solution. Otherwise the distance formula (Eqn. 9) was applied to the intersection points to yield path length, S.

[9] $$S = \sqrt{(x_2 - x_1)^2 + (y_2 - y_1)^2 + (z_2 - z_1)^2}$$

Norman and Welles (1983) have also computed the solution for the intersection of a ray with an ellipsoid.

Since absorbance is the product of foliage projection, path length and density (Eqn. 10), A was divided by the foliage projection value, $G[Z,x]$, for this solar zenith and species combination (see below) and by the length of the light path through the crown (S), yielding the crown foliage area density (F, Eqn. 11). Note that this sampling technique includes the within-crown bole and branches as part of the crown foliage. Foliage densities were averaged over all measurement points within each tree's shadow, then over all trees. Since ellipsoidal crowns were sampled by radial transects, the within-tree average was weighted by the length from the transect origin to the measurement point to even out the area sampling rate.

[10] $$A = G[Z,x]SF$$

[11] $$F = \frac{A}{G[Z,x]S}$$

Foliage inclination

Single-tree light transmission data obtained at a number of solar angles were provided by Constabel (1995). She measured 10 aspen, 10 overstory white spruce and 10 understory white spruce trees on June 22, 1994 in a partial-cut mixedwood site near Edson, Alberta (53°40' N, 116°40' W). Shadows were sampled during five one-hour periods with mean solar zenith angles of 30.7°, 32.9°, 35.7°, 51.2° and 65.3°. In the crown shadow of each tree, nine measurements (Q) were taken with the radiometer wand held parallel to the bole. Three measurements were taken in the upper third of the crown, three in the middle, and three in the lower third, then averaged for each tree. Total (Q_0) and diffuse irradiance ($Q_{diffuse}$) were measured in full sun adjacent to the crown shadow immediately before and after sampling each tree as outlined for the foliage area density measurements above. Tree height, h_t, live-crown height, h_{lc}, and crown width, cw, were determined with a clinometer and measuring tape.

We calculated direct-beam light absorbance by the crown, A, from this data by subtracting the diffuse component and inverting Eqn. 1 as above (Eqn. 8). Since the measurement points were not mapped spatially (to speed up sampling), we had to simplify the crown shape. We first determined the volume of each crown as either an ellipsoid (aspen) or a rocket (white spruce) using the crown length and width to establish the axis lengths. We then redefined the crowns as rectangular solids with one side facing the sun, one crown length deep and of equal length and width (w) such that they contained the same volume as the original shape. The path length of light through the crown, S, at each solar zenith was calculated using the width (w) of the rectangle (Eqn 12).

[12] $$S = \frac{w}{\sin Z}$$

Crown absorbance, A, was then divided by the path length, S, to yield absorbance per unit length (A/S).

Campbell and Norman (1989) showed that the inclination of foliage with random azimuth orientation can be efficiently and flexibly modeled as the surface of an ellipsoid. The only

parameter required by this distribution is the ratio of vertical to horizontal foliage projections of the ellipsoid, $x_{projection}$ (Eqn. 13).

$$[13] \quad G[Z, x_{projection}] = \frac{\sqrt{x_{projection}^2 \cos^2 Z + \sin^2 Z}}{(x_{projection} + 1.774(x_{projection} + 1.182)^{-0.733})}$$

The projection ratio, $x_{projection}$, and the foliage area density, F, can be obtained by least-squares non-linear regression of light absorbance per unit length (A/S) on the solar zenith (Z, Eqn. 14). We used the derivative-free secant nonlinear regression method available in PROC NLIN, SAS release 6.12 (SAS Institute, Cary, NC).

$$[14] \quad A/S = G[Z, x_{projection}]F$$

The parameters $x_{projection}$ and F were calculated for each tree, then averaged for the species. Since the measurement points were not well-mapped, only the projection ratio ($x_{projection}$) was used.

The MIXLIGHT Model

Crown-scale modeling

The light transmission model was adapted from previous models developed in Scandinavia (Pukkala et al. 1993) and New England (Canham et al. 1994). The trees were projected mathematically in 3-dimensional (x, y, z) space with paraboloid stems truncated at the base of the crown and crowns of the shape appropriate to the species (ellipsoids, paraboloids, cylinders, cones or rockets). The elevations of the stems and crowns were adjusted for the stand slope and aspect.

At each measurement point, diffuse skylight transmission was calculated by averaging the transmission along 480 light paths (24 equally spaced azimuth angles (na) from 0 to 360°, and 20 zenith angles (nc), spaced by equal increments of the cosine of the zenith from 1 (cos 0°) to 0 (cos 90°); Eqn. 3b). Each path was checked for slope, bole and crown hits. If the light source was obscured by the sloping ground (Eqn. 15), a value of 0% light transmission was returned for that path.

$$[15] \quad \cos(r \wedge r_s) = \cos\beta\cos Z + \sin\beta\cos(\alpha - \Omega)$$

In Eqn. 15, $\cos(r \wedge r_s)$ is the cosine of the angle between a line perpendicular to the slope and the light source, β is the slope inclination, and Ω the slope aspect. If $\cos(r \wedge r_s)<0$, the source is obscured by the slope. Bole hits were determined by checking the paraboloid stems for an intersection with the light path using the same simultaneous solutions to the ray and paraboloid equation as used in the calibration. Bole hits also returned 0% transmission for that path. In the absence of these, ray transmission was determined by the length the light ray passed through crowns of the various species between the simulation point and the sky. Again, the simultaneous solution to the ray and crown equation was used to determine intersection points and Eqn. 9 applied to obtain the distance. The length of the ray through each tree encountered was multiplied by the foliage projection and foliage area density for the appropriate species to give an absorbance ($A_j = G[Z,x_j]S_jF_j$), which was summed for all crowns encountered on the path. The sum of these absorbance values along each light path was then converted back to a flux density by Eqn. 2. We used the uniform overcast sky (UOC) assumption for diffuse light: incident light from all equal-area sectors of the sky was assumed to have equal flux density in the diffuse light calculation, *i.e.* $q_0[Z,\alpha]=1$ for all Z,α.

Direct sunlight absorbance was obtained in a similar way, but for only one light path using the solar zenith and azimuth angles at the date, time and location of measurement (Iqbal 1983). The proportions of direct and diffuse light at the time of measurement were applied to the output to give the predicted total light transmission.

Canopy-scale modeling

To avoid excessive edge effects, crown scale modeling requires that a large area of trees must be mapped and predictions made for an small area in the center. This allows light transmission at large zenith angles to be calculated without encountering the plot edge. In smaller inventory plots, evaluation of light rays would be restricted to limited angles. A 50 × 50 m inventory plot, for example, allows a maximum zenith of 51° from its center if the trees are 20 m tall. Although the light path transmission values are weighted by the cosine of their zenith angle, 40% of the weight of the diffuse or seasonal light measurement would be obtained from zenith angles larger than 51°.

Light transmission is low at large zenith angles owing to the long path through the canopy, so ignoring these angles would inflate the transmission estimate.

When edge effects are large, or when the input data lack a stem map, a model based on a single canopy rather than individual crowns is more appropriate. The canopy is assumed to be infinite in horizontal extent (or up, down and cross-slope), as tall as the average canopy tree, and with foliage randomly distributed throughout. The canopy foliage area density (F_{canopy}) is the sum of the leaf area (the product of crown volume, V_{ij}, and crown foliage density, F_i) and one side of the below-crown bole surface area (B_{ij}) borne by all trees (j) of all species (i), divided by the canopy volume (V_{canopy}) (Eqn. 16a,b):

$$[16a] \quad F_{canopy} = \frac{\sum_{i=1}^{nspecies} \sum_{j=1}^{ntrees} \left(V_{ij} F_i + \frac{1}{2} B_{ij} \right)}{V_{canopy}}$$

$$[16b] \quad V_{canopy} = plot\ length \times plot\ width \times average\ canopy\ tree\ height \times \cos\beta$$

where β is the slope inclination. The volumes of the geometric crowns and the surface area of the paraboloid boles (B_{ij}) was calculated using standard equations (Glover 1996).

The projection of a unit of canopy foliage ($G_{canopy}[Z]$) was determined at each zenith angle as the projected area of the foliage (crown volume × foliage area density × projection) and the below-crown bole of each tree of each species, divided by the total foliage and bole area (F_{canopy}, Eqn 17a,b). We simplified the bole projection to the projection of a parabola with one face to the light source. This underestimates the projected area significantly only for very small zenith angles.

$$[17a] \quad G_{canopy}[Z] = \frac{\sum_{i=1}^{nspecies} \sum_{j=1}^{ntrees} (V_{ij} F_i G[Z, x_i] + \frac{4}{3} r_{ij} h_{ij} \sin Z)}{F_{canopy}}$$

$$[17b] \quad r_{ij} = \sqrt{\frac{dbh_{ij} h_{ij}}{2(h_{ij} - 1.3)}}$$

Here, r_{ij} is the radius at the base of the paraboloid bole, dbh_{ij} is the bole diameter at 1.3 m height, and h_{ij} is the tree height.

Light transmission is calculated as for the crown-scale model, except that the one light-absorbing region makes calculating the path length much simpler. If the canopy is the height of an average canopy tree (h_{cznopy}) and extends 'horizontally' (following the ground slope) to infinity, path length (S_{canopy}) is given by Eqn. 17:

$$[18a] \quad S_{canopy} = \frac{(h_{canopy} - z_o)\cos\phi}{\cos(Z - \phi)}$$

$$[18b] \quad \phi = \arctan[\tan\beta\cos(\alpha - \Omega)]$$

where z_o is the height of the measurement point, Z and α are the zenith and azimuth of the light path, ϕ is the apparent slope in the α direction, and the slope inclination, β, and aspect, Ω, are as measured in the stand inventory.

Daily and Seasonal Modeling

The prediction calculations shown above are for instantaneous predictions at a particular time of day and season. MIXLIGHT is also capable of modeling light transmission over an entire day, season, or year. This is done with an algorithm that builds a 'seasonal sky' (or daily sky) for the time interval of interest. The algorithm follows Canham et al. (1994), combining the estimates of diffuse and direct radiation into a fraction of the total seasonal flux density for each equal-area sector of the sky. Eqn. 3b is then applied to all sectors of the sky, but using these fractional flux density values as the incident flux density ($q_0[Z, \alpha]$). The final averaged transmission value estimates seasonal transmission. This is much more efficient than recalculating transmission for every hour of the day over the desired time inverval.

Stand Level Validation

Alberta Forest Service Permanent Sample Plots (PSPs) were used to apply and test the instantaneous predictions of MIXLIGHT on a stand level. We selected 17 upland PSPs, with species compositions ranging from dominance by pure aspen, white spruce, or lodgepole pine, to mixtures of these and balsam poplar, white birch and balsam fir. Stand density varied from 335 to 1420 stems ha^{-1}, and stand age (all sites were fire-initiated) from 69 to 159 years. We sampled 16

plots during the deciduous leaf-on period (mid June - early September) in 1996 and 1997, and remeasured 8, as well as 1 new one, in the leaf-off period (April 1997). Light measurements were made with the same linear radiometer as the calibration measurements, either during uniformly cloudy (no direct sunlight) or uniformly clear (most light from the sun) periods. Light was sampled above shrub height (~1.5 m) for 36-49 points following a 5 × 5 m pattern. At each point, 12 light readings were taken at 30° increments while sweeping the radiometer wand around a horizontal circle at arm's length: the mean of these 12 flux density measurements was recorded. These values were expressed as a percentage of the 5-minute floating average of above-canopy light at the same time, which was measured by a point quantum sensor (LI-190SA, Li-Cor, Lincoln, NB) and datalogger (CR21X Campbell Scientific, Logan, UT) in a nearby clearing. These 36-49 transmission measurements were then averaged to give the stand-level light transmission value.

On sunny days, the proportion of diffuse light was determined by sampling a single radiometer sensor outside the stand with and without a shade disk before and after the plot measurements, as in the calibration measurements. Trees were tallied to check for new mortality or ingrowth since the last Forest Service inventory, and measurements were taken of height, live-crown height, crown radius and breast-height diameter (DBH) for 8-12 trees in the plot. A polynomial regression between these crown parameters and DBH, overstory species density and composition was developed for each species. For each PSP, we then created a complete list of all the trees, containing species, status, stem position (x and y coordinates), DBH, and estimated height, height-to-live-crown, and crown radius for each tree. The tree lists were loaded into the model along with the appropriate site information (latitude, longitude, slope, aspect, plot dimensions, date and time of measurement, percentage of diffuse light at time of measurement). Canopy-scale model predictions were then compared to the measured values of light transmission on a stand-average basis.

Model Sensitivity and Foliage Inclination

The model was evaluated for the sensitivity of its light transmission predictions to the inputs on a stand level. This sensitivity analysis was performed on 3 stand types: deciduous-dominated, mixed

conifer-deciduous with some large ($80m^2$) gaps, and a conifer stand. For each sensitivity run, we altered one of the 4 key parameters for all species: the foliage area density (F), the ellipsoidal leaf inclination parameter ($x_{projection}$), the crown radius (cr), and the crown length (cl). The parameters were varied through a set of logarithmic multiples over seven runs: 2^{-2}, 2^{-1}, $2^{-0.5}$, 2^{0}, $2^{0.5}$, 2^{1}, and 2^{2} (25, 50, 71, 100, 141, 200, and 400% of the original value). Light transmission predictions were compared across this range.

Since a number of other models have not attempted to account for the effects of foliage inclination (Pukkala et al. 1993, Canham et al. 1994), and work is required to calibrate this parameter, we also ran MIXLIGHT on the validation sites with the foliage inclination set to spherical ($x_{projection}=1$) for all species. This also meant small changes in the foliage area density estimates, since they were also corrected for inclination during calibration.

Results

Calibration

Calibration trees were sampled in 10 harvested areas. Generally, each species was sampled at least at two different sites, except for lodgepole pine for which only one suitable cutblock was available. Tree size spanned the range of sizes which might be expected in mature stands (Table 1). Selection of the appropriate geometric crown shape was straightforward. Early self-pruning and die-back of the lower branches made an ellipsoid shape appropriate for the deciduous and pine crowns. Continuous branch growth with the development of a slight sag made a paraboloid fit the fir crowns well, and the rocket (cone over cylinder) shape was superior for white spruce because of the increasingly pronounced branch sag from the mid to lower crown.

Individual fir crowns transmitted the least light, followed by overstory white spruce, understory spruce, pine, and leaf-on birch, aspen, and balsam poplar (Table 1). During the leaf-off season, light transmission through deciduous crowns was roughly doubled. In 50 of the 57 trees sampled, and without apparent bias as to species or size, the light absorption value calculated at each measurement point within the crown shadow was significantly correlated with the calculated path length of sunlight through the geometric crown to that point (data not shown), indicating that path length can account for at least some of the variation in transmitted light. Regression analysis indicated that the effect of path length (S) on light absorbance (A) was linear, so Eqn. 10 would provide an appropriate fit, with $G[Z,x]F$ as the slope.

Crown foliage area densities generally followed similar patterns as crown light transmission: species that transmitted little light through their crowns had the highest foliage density (Table 1). That this is not necessarily so is shown by birch, which, owing to the short light path through its narrow crown, transmitted more light than aspen, yet had more foliage per unit crown volume. There was no effect of bole diameter or crown volume on the foliage density within each species (data not shown). Foliage inclination, measured in leaf-on aspen and white spruce only, tended from mostly vertical for overstory spruce (0.10 as much straight-down as sideways projection) to 0.53 for understory spruce, to close to spherical (x=0.82) for aspen (Table 1).

Table 1. Calibration trees' bole and crown parameters. Data shown are minimum-maximum (mean).

Species[1]	Season	# of trees	DBH (cm)	Height (m)	Crown length (m)	Crown radius (m)	Crown shape	Crown light transmission (%)	Crown foliage area density (m^2m^{-3})	Ellipsoidal inclination parameter $(x_{projection})^2$
Fb	leaf-on	3	12-23 (17)	8.7-15.5 (11.6)	3.6-7.8 (5.6)	1.5-2.1 (1.8)	paraboloid	9-14 (12)	1.896-2.064 (1.980)	1
Sw overstory	leaf-on	5	39-67 (48)	20.1-28.9 (26.0)	5.9-12.1 (9.7)	1.2-2.2 (1.7)	rocket	5-28 (19)	1.317-2.562 (1.875)	0.10
Sw understory	leaf-on	5	13-20 (16)	6.7-11.8 (9.4)	3.4-5.9 (4.6)	1.4-2.1 (1.7)	rocket	6-45 (24)	0.811-2.619 (1.796)	0.53
Pl	leaf-on	6	18-28 (23)	18.2-23.7 (20.9)	2.1-4.5 (3.3)	0.7-1.5 (1.2)	ellipsoid	23-33 (27)	1.030-1.860 (1.394)	1
Aw	leaf-on	11	25-62 (43)	21.3-28.5 (24.0)	3.4-8.9 (6.5)	1.5-4.1 (3.0)	ellipsoid	22-53 (36)	0.245-0.682 (0.442	0.82
Bw	leaf-on	7	8-31 (15)	9.1-24.0 (13.2)	2.8-10.3 (5.8)	1.2-3.5 (2.0)	ellipsoid	20-55 (39)	0.312-1.770 (0.804)	1
Pb	leaf-on	6	12-47 (39)	8.5-27.1 (21.8)	2.9-10.0 (6.3)	1.2-3.1 (2.3)	ellipsoid	40-59 (52)	0.166-0.638 (0.298)	1
Aw	leaf-off	6	25-48 (36)	22.3-26.3 (23.6)	2.5-6.5 (5.2)	1.6-3.3 (2.6)	ellipsoid	66-87 (74)	0.090-0.192 (0.138)	1
Bw	leaf-off	5	7-31 (20)	8.2-23.6 (14.9)	3.2-9.3 (5.7)	1.9-3.5 (2.4)	ellipsoid	70-93 (78)	0.042-0.222 (0.124)	1
Pb	leaf-off	3	12-47 (31)	9.8-24.8 (18.5)	2.7-5.0 (4.1)	0.8-3.0 (2.0)	ellipsoid	74-84 (77)	0.118-0.232 (0.170)	1

[1]Species codes: Fb = balsam fir, Sw = white spruce, Pl = lodgepole pine, Aw = trembling aspen, Bw = white birch, Pb = balsam poplar.

[2]Parameter describing the relative projection of leaf area in the vertical *vs.* the horizontal direction assuming the leaves follow an ellipsoidal inclination distribution (Campbell and Norman 1989). Calibrated for the dominant trees, aspen (leaf-on, n=10), overstory (n=10) and understory white spruce (n=10), only using the data of Constabel (1995); all other species are assigned the default value of 1 (foliage area inclined as if covering the surface of a sphere).

Validation

MIXLIGHT predictions of instantaneous stand-level light transmission were well-correlated with measured light transmission (Fig. 2, Pearson's r=0.86, n=25, P<0.0001). The slope of the predicted *vs.* measured relationship (1.03) for a regression constrained to pass through the origin was not significantly different from the ideal slope of 1 (P=0.5606). For some medium-light sites, MIXLIGHT predicted higher light levels than were actually measured by as much as 22% absolute transmission (44% transmission predicted for a site with 22% measured light). There was also a tendency to underestimate transmission to high-light sites (which were measured under leaf-off conditions): the worst was 48% transmission predicted for a site in which 64% was measured. The residual plot suggests a curvilinear relationship (Fig. 2b); indeed, linear and quadratic equations with intercepts had a better fit (R^2=0.75 and 0.82, respectively) than the linear, zero-intercept equation (R^2=0.70). Analysis of the residuals from a 1:1 relationship showed that the deviations were negatively correlated with increasing site moisture class: overstory light

transmission tended to be overestimated in wetter sites and underestimated in drier sites (P=0.0065). No effect of site nutrient status was detectable (P=0.6194).

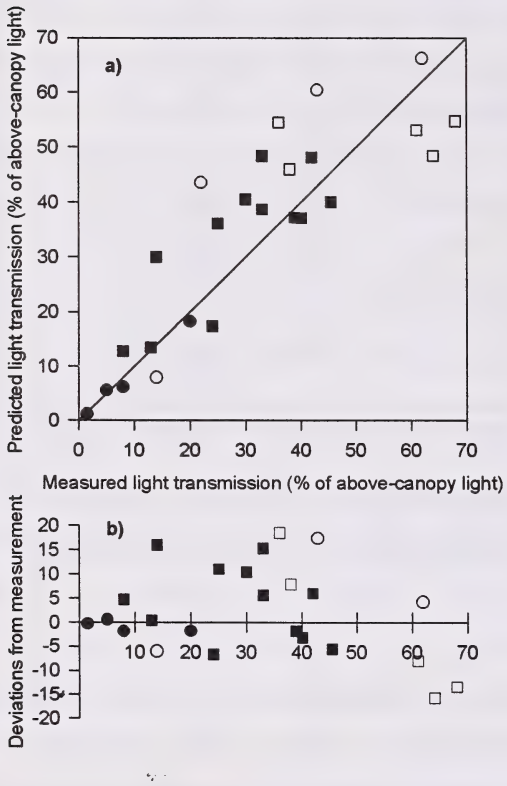

Figure 2. MIXLIGHT stand-level validation for 17 sites measured and modeled under various weather conditions and seasons: ○leaf-off on a sunny-day, □leaf-off on a cloudy day, ●leaf-on on a sunny day, ■leaf-on on a cloudy day. a) Predicted instantaneous light transmission (% of above-canopy light) is compared to measured light transmission averaged across the stand. b) Residuals from a 1:1 relationship between predicted and measured light transmission. Since some sites were measured under several conditions (sun/cloud, leaf-on/leaf-off) there are 25 data points.

Sensitivity Analysis and Foliage Inclination

Results of the sensitivity analysis of MIXLIGHT at the canopy level were similar under sunny and cloudy conditions. Only the overcast-day results, which had slightly more variation, are shown (Fig. 3). Predictions were most responsive to foliage area density and crown radius. Doubling or halving the species' foliage densities (the range indicated by the calibration data) caused a change

in the light prediction of about half the base transmission value in the aspen and mixedwood stands, and slightly more in the spruce stand. Crown radius had an effect on transmission roughly similar in magnitude to foliage density, but more asymmetric. An increase in radius tended to have a greater effect than a decrease, except in the spruce stand where the change was equal. The effect of varying the tree crown length was always smaller than the effect of varying foliage density. Varying the foliage inclination parameter ($x_{projection}$) caused the least effect: even extreme (¼-4×) variations (*e.g.* $x_{projection}$ =0.026-0.42 for canopy spruce and $x_{projection}$ =0.20-3.3 for aspen) caused a change in the predicted transmission of only a relative 20% from base transmission value.

The results of assuming the foliage inclination was spherical for all species are shown in Fig. 4. Light in all sites was underestimated, but the relative error was particularly high for the low-light sites. Model predictions are still precise and actually capture more of the site-to-site variation (adjusted R^2=0.78, *vs.* 0.66 when the measured foliage inclination parameters were used), but consistently predict lower values.

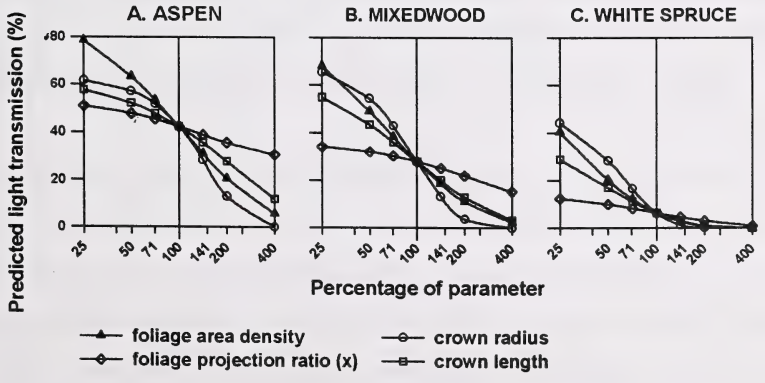

Figure 3. Sensitivity analysis of the foliage area density, foliage inclination, and crown length and radius parameters that drive MIXLIGHT for three stands: a) Aspen-dominated, b) White spruce / Aspen Mixedwood (with gaps), c) White spruce-dominated. Light transmission predictions are instantaneous canopy-level predictions for a cloudy day in midsummer.

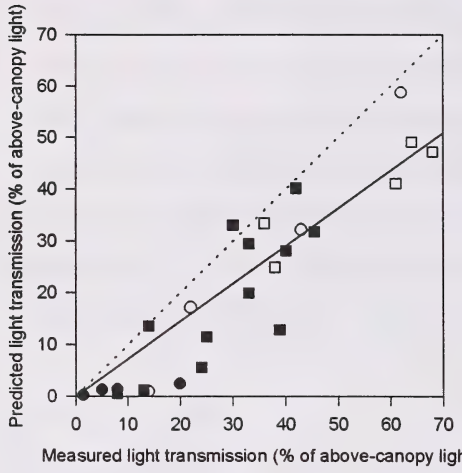

Figure 4. MIXLIGHT stand-level validation for the same 17 sites as Fig. 2 but with foliage inclination assumed to be spherical ($x_{projection}$=1). Sites were measured and modeled under various weather conditions and seasons: ○leaf-off on a sunny-day, □leaf-off on a cloudy day, ●leaf-on on a sunny day, ■leaf-on on a cloudy day. Predicted instantaneous light transmission (% of above-canopy light), with the foliage inclination parameter set to 1 for all species, is compared to measured light transmission averaged across the stand. The dotted line is the 1:1 relationship.

Discussion

On a canopy scale, MIXLIGHT predicts light transmission very well for a wide range of stands during leaf-on and leaf-off seasons and under sunny and cloudy conditions (Fig. 2). Validation stands varied from highly structured mixtures of tree species with patches and gaps to closed, single-species, single-strata canopies. It appears that MIXLIGHT can capture much of the site-to-site variation in light transmission based on inventory data and the two species-specific calibration parameters. It should thus be an effective modeling tool for managing understory regeneration and vegetation in extensive forest areas.

There are many models available for predicting light transmission in mature forests (*e.g.* Norman and Jarvis 1975, Grace et al. 1987, Wang and Jarvis 1990, Pukkala et al 1993, Canham et al. 1994, Cescatti 1997a). However, with the exception of Canham et al. (1994), these have been developed and tested in one or two single-species stands and require extensive data collection in each stand for calibration. The crown-scale model of MIXLIGHT is similar in principle to the models of Pukkala et al. (1993) and Canham et al. (1994), but is simpler to calibrate, and incorporates boles, a greater variety of crown shapes, and accounts for foliage inclination. The canopy model, which is validated with independent measurements in this paper, makes it possible to apply MIXLIGHT extensively to sites with a very limited set of data.

For canopy-scale modeling MIXLIGHT requires only a list of species, bole diameter, height and crown dimensions (length and width), which are usually available in standard forest inventory plots, and species-specific foliage inclination and projection parameters. Bole diameter to height functions are available for tree species in many forest districts; we were also able to develop reasonable diameter to crown length relationships based on stand characteristics. A predictive function for crown width or radius has proved more elusive. This parameter is affected by snow and wind through crown abrasion (Grier 1988), as well as by stand density and composition. Good within-stand relationships were calibrated using bole diameter and as predictive variables, but we are currently collecting more extensive data on crown width in hopes of developing a better predictor. In principle, these relationships could reduce MIXLIGHT data requirements to

the two foliage parameters, site attributes (size, canopy height, slope, aspect) and a list of species and bole diameter.

Leaf area, the most critical driving variable in MIXLIGHT (Fig.3) and other light transmission models (Sampson and Smith 1993), is also one of the most difficult parameters to measure. Allometric equations are commonly used to relate leaf area to bole diameter or sapwood area (Pierce and Running 1988, Pukkala et al. 1993) but require considerable effort to calibrate. Branch and bole area must be also be estimated, as these also extinguish light. Light interception techniques (Welles and Cohen 1996) provide a simpler method to estimate shading leaf, branch and bole area, but have generally been applied to entire canopies. However, Lang and McMurtrie (1992), Acock et al. 1994) and Villalobos et al. (1995) determined foliage area density or foliage area index using these methods on individual plants. Lang and McMurtrie (1992) and Acock et al. (1994) found these methods tended to underestimate foliage area, and more so if a linear radiometer was used rather than the LI-COR plant canopy analyzer (LAI-2000, LI-COR, Lincoln, NB) (Acock et al. 1994). Lang and McMurtrie (1992) attributed this underestimation to non-random foliage distribution in these small (<1.3 m tall) plants. Villalobos et al. (1995) found reasonable estimation of single-tree foliage area using a plant canopy analyzer with larger olive trees. Our calibration trees had large crowns and all species demonstrated a linear relationship between direct-beam light absorbance (the negative logarithm of direct-beam light transmission) and path length, a consequence of a random foliage distribution. We did not independently verify our foliage density estimates, but our data met the theoretical requirements for the light interception technique to work.

Our leaf-on foliage area estimates are higher than values reported for other species. Pukkala et al. (1993) report projected leaf area density (*i.e.* $F_{proj}=G[Z]F$) and Canham et al. (1994) report 'absolute path length extinction coefficients' which are mathematically equivalent to projected foliage area density. This parameter can be obtained from our calibration data by dividing direct-beam light absorbance by path length (Eqn. 10) and assuming the projection ($G[Z]$) remains constant for all light source angles, Z (*i.e.* a spherical distribution of foliage inclination angles (Oker-Blom 1986)). Our average projected foliage density for lodgepole pine was 0.697 m^2m^{-3}

while Pukkala et al. (1993) reported values of about 0.4 m^2m^{-3} for Scots pine of similar size. The range of F_{proj} for New England species was 0.066 m^2m^{-3} for red oak (*Quercus rubra* L.) to 0.322 m^2m^{-3} for white pine (*Pinus strobus* L.) while the range for our boreal species was 0.199 m^2m^{-3} for balsam poplar to 0.990 m^2m^{-3} for balsam fir. The differences appear to be due to smaller, denser crowns in our boreal species.

In several validation sites, MIXLIGHT's prediction error for stand-level light transmission was nearly half the measured value. This error may be important where the goal is to determine critical light levels for the survival of particular species. Fortunately, errors of this magnitude occurred for medium to high-light sites (>14% transmission) rather than low-light sites where the relative error would be greater and where the light compensation points of tree and understory species occur (*e.g.* Greenway 1994, Man and Lieffers 1997). The sensitivity analysis indicated that the prediction range for the variation found in the foliage area density parameter was similar in magnitude to the largest prediction error for the validation (Table 1 and Fig. 3). No trends were found between foliage density and tree size or site nutrient status; however, deviations from the measured values were correlated with site moisture index. Since leaf area for aspen in particular appears to be limited by moisture (Waring and Schlesinger 1985, Messier et al. 1998), it is not surprising that wetter sites transmit less light than was predicted using the foliage area density of an 'average' tree. Fine-tuning improvements to MIXLIGHT could be made by further calibration of the species' foliage area densities for sites of different moisture index.

Light scattering may provide another source of error in the estimation of foliage area and subsequent simulation of light transmission. We assumed that the foliage elements transmit and reflect no light, but clearly this is not the case. For calibration, most of the effect of scattered light was removed by sampling the diffuse light in a sunlit area immediately next to the tree. Subtracting this diffuse flux from the light flux density values measured within the crown shadow left the direct sunlight component required for determining the foliage parameters, assuming the diffuse (including scattered light) component was evenly distributed about the tree. Error was introduced to the extent that this was not true. For simulating light penetration through crowns or a canopy, neglecting light scattering should result in underestimation of the actual light

transmission. That this is not apparent suggests that scattering is a smaller component than other noise in the MIXLIGHT canopy model.

Although canopy-scale modeling is more rapid and does not require a stem map, the assumption of random foliage distribution throughout the canopy volume is one which may not be met. The most obvious level of foliage grouping is into crowns. This grouping means that in open stands, as might occur following partial-cutting, more light penetrates to the ground surface than would be predicted by a model that spreads the foliage randomly throughout the site. Crown-scale modeling may be more appropriate for these situations.

The sensitivity analysis illustrates the behavior of MIXLIGHT under systematic changes to its key parameters. It is clear that foliage area density and crown radius should be most carefully estimated. Crown length and inclination are less critical, particularly if only a relative site-to-site comparison is required. If accurate predictions are required, however, it is clear that even foliage inclination should be well estimated since setting the foliage inclination to spherical for the validation sites created a substantial downward bias in the predictions.

Conclusions

MIXLIGHT provides a flexible predictive light transmission model for evaluating stand tending and silvicultural options. Calibration of species' foliage area density and inclination parameters is easily performed using residual trees in recent cutblocks. Instantaneous stand-level predictions were well-correlated with measurements of light transmission. Work is currently under way to evaluate the microsite-level predictability of MIXLIGHT on both an instantaneous and long-term basis. Copies of BASIC code for MIXLIGHT are available from the authors.

Literature Cited

Alaback, P.B. and J.C. Tappeiner II. 1991. Response of western hemlock (*Tsuga heterophylla*) and early huckleberry (*Vaccinium ovalifolium*) seedlings to forest windthrow. Canadian Journal of Forest Research 21: 534-539.

Anonymous. 1982a. Canadian Climate Normals, Vol. 2. Temperature. Environment Canada, Atmospheric Environment Service, Downsview, Ontario, 306 pp.

Anonymous. 1982b. Canadian Climate Normals, Vol. 3. Precipitation. Environment Canada, Atmospheric Environment Service, Downsview, Ontario, 602 pp.

Anonymous. 1994. Ecological Land Survey Site Description Manual. Alberta Environmental Protection, Edmonton, Alberta, 166 pp.

Campbell, G.S. and J.M. Norman. 1989. The description and measurement of plant community structure. In Plant canopies: their growth, form, and function (G. Russell, B. Marshall and P.G. Jarvis, eds) - Society for Experimental Biology Seminar Series 31, pp. 1-19.

Canham, C.D., A.C. Finzi, S.W. Pacala, and D.H. Burbank. 1994. Causes and consequences of resource heterogeneity in forests: interspecific variation in light transmission by canopy trees. Canadian Journal of Forest Research 24: 337-349.

Cescatti, A. 1997a. Modeling the radiative transfer in discontinuous canopies of asymmetric crowns. I. Model structure and algorithms. Ecological Modeling 101: 263-274.

Cescatti, A. 1997b. Modeling the radiative transfer in discontinuous canopies of asymmetric crowns. II. Model testing and application in a Norway spruce stand. Ecological Modeling 101: 275-284.

Constabel. A.C. 1995. Light Transmission Through Boreal Mixedwood Stands. M.Sc. Thesis, Department of Forest Science, University of Alberta, Edmonton, Alberta, Canada, 73 pp.

Glover, T.J. 1996. Pocket Ref. Sequoia, Littleton, CO, 542 pp.

Grace, J.C., P.G. Jarvis, and J.M. Norman. 1987. Modeling the interception of solar radiant energy in intensively managed stands. New Zealand Journal of Forestry Science 17: 193-209.

Greenway, K.J. 1994. PhD thesis, University of Alberta, Edmonton, Alberta.

Grier, C.C. 1988. Foliage loss due to snow, wind, and winter drying damage: its effects on leaf biomass of some western conifers. Canadian Journal of Forest Research 18:1097-1102.

Iqbal, M. 1983. An Introduction to Solar Radiation. Academic Press, New York, 390 pp.

Klinka, K., Q. Wang, G.J. Kayahara and R.E. Carter. 1992. Light-growth response relationships in Pacific silver fir (*Abies amabilis*) and subalpine fir (*Abies lasiocarpa*). Canadian Journal of Botany 70: 1919-1930.

Lieffers, V.J., C. Messier, K.J. Stadt, F. Gendron, P.Comeau. 1998. Predicting and managing light in the understory of boreal forests. Submitted to the Canadian Journal of Forest Research.

Lieffers, V.J. and K.J. Stadt. 1994. Growth of understory *Picea glauca, Calamagrostis canadensis,* and *Epilobium angustifolium* in relation to overstory light transmission. Canadian Journal of Forest Research 24: 1193-1198.

Man, R. and V.J. Lieffers. 1997. Seasonal photosynthesis responses to light and temperature in white spruce (*Picea glauca*) seedlings planted under an aspen (*Populus tremuloides*) canopy and in the open. Tree Physiology 17: 437-444.

McLure, J.W. and T.D. Lee. 1993. Small-scale disturbance in a northern hardwoods forest: effects on tree species abundance and distribution. Canadian Journal of Forest Research 23: 1347-1360.

Messier, C. T.W. Honer, and J.P. Kimmins. 1989. Photosynthetic photon flux density, red:far-red ratio, and minimum light requirement for survival of *Gaultheria shallon* in western red cedar - western hemlock stands in coastal British Columbia. Canadian Journal of Forest Research 19: 1470-1477.

Messier, C., Parent, S. and Bergeron, Y. 1998. Characterization of understory light environment in closed mixed boreal forests: effects of overstory and understory vegetation. J. Veg. Science. In press.

Norman, J.M. and P.G. Jarvis. 1975. Photosynthesis in Sitka spruce (*Picea sitchensis* (Bong.) Carr.) V. Radiation penetration theory and a test case. Journal of Applied Ecology 9: 747-766.

Norman, J.M. and J.M. Welles. 1983. Radiative transfer in an array of canopies. Agronomy Journal 75: 481-488.

Oker-Blom, P. 1986. Photosynthetic radiation regime and canopy structure in modeled forest stands. Acta Forestalia Fennica 197: 1-44.

Oker-Blom, P., M.R. Kaufmann, and M.G. Ryan. 1991. Performance of a canopy light interception model for conifer shoots, trees and stands. Tree Physiology 9: 227-243.

Pierce, L.L. and S.W. Running. 1988. Rapid estimation of coniferous forest leaf area index using a portable integrating radiometer. Ecology 69: 1762-1767.

Poage, N.J. and D.R. Peart. 1993. The radial growth of American beech (*Fagus grandifolia*) to small canopy gaps in northern hardwood forest. Bulletin of the Torrey Botanical Club 120: 45-48.

Poulson, T.L. and W.J. Platt. 1989. Gap light regimes influence canopy tree diversity. Ecology 70: 553-555.

Pukkala, T., T. Kuuluvainen, and P. Stenberg. 1993. Below-canopy distribution of photosynthetically active radiation and its relation to seedling growth in a boreal *Pinus sylvestris* stand: a simulation approach. Scandinavian Journal of Forest Research 8: 313-325.

Runkle, J.R. G.H. Stewart, and T.T. Veblen. 1995. Sapling diameter growth in gaps for two *Nothofagus* species in New Zealand. Ecology 76: 2107-2117.

Sampson, D.A. and F.W. Smith. 1993. Influence of canopy architecture on light penetration in lodgepole pine (*Pinus contorta* var. *latifolia*) forests. Agricultural and Forest Meteorology 64: 63-79.

Ter-Mikaelian, M.T., R.G. Wagner, C. Shropshire, F.W. Bell, and C.J. Swanton. 1997. Using a mechanistic model to evaluate sampling designs for light transmission through forest canopies. Canadian Journal of Forest Research 27: 117-126.

Wang, Y.P. and P.G. Jarvis. 1990. Description and validation of an array model - MAESTRO. Agricultural and Forest Meteorology 51: 237-280.

Waring, R.H. and Schlesinger, W.H. 1985. Forest Ecosystems: concepts and management. Academic Press, New York.

Welles, J.M and S. Cohen. 1996. Canopy structure measurement by gap fraction analysis using commercial instrumentation. Journal of Experimental Botany 47: 1335-1342.

Appendix A

Light ray equation:

Equation of a line containing the measurement point (x_0, y_0, z_0), and with vertical (zenith) angle, Z, and orientation with respect to north (azimuth), α:

$$x = x_0 + t\sin\alpha$$

[A1] $$y = y_0 + t\cos\alpha$$

$$z = z_0 + t\cot Z$$

where t is any real number.

Crown and bole shape equations:

Crowns are truncated at the bottom at the tree base elevation plus the live-crown height ($z_b + h_{lc}$) and at the top at base elevation plus tree height ($z_b + h_t$). Crown centers are at the point (u, v, w) where u and v are the x- and y-coordinates of the tree base (x_b, y_b), and $w = z_b + h_{lc} + \frac{1}{2}cl$ and $cl = h_t - h_{lc}$. Boles are truncated at the tree base elevation (z_b) at the bottom and the live crown height ($z_b + h_{lc}$) at the top. For calibration of the foliage area density and inclination parameters, the point (0, 0, 0) was set to the center of the crown shadow. For predicting light in a stand, the point (0, 0, 0) was set to the center of the stand.

Cylinder:

[A2] $$(x-u)^2 + (y-v)^2 = cr^2$$

Cone:

[A3] $$(x-u)^2 + (y-v)^2 = \left[cr - \tfrac{cr}{cl}(z - h_{lc})\right]^2$$

Rocket:

Cylinder equation from $z = (z_b + h_{lc})$ to $z = (z_b + h_{lc} + \frac{3}{4}cl)$

Cone equation from $z = (z_b + h_{lc} + \frac{3}{4}cl)$ to $z = (z_b + h_t)$.

Paraboloid:

[A4] $$(x-u)^2 + (y-v)^2 = -\tfrac{cr^2}{cl}(z-h)$$

Ellipsoid:

[A6] $$\frac{(x-u)^2}{cr^2} + \frac{(y-v)^2}{cr^2} + \frac{(z-w)^2}{(cl/2)^2} = 1$$

National Library of Canada
Bibliothèque nationale du Canada
3 3286 51614 8455